Submitted to The Astrophysical Journal
Preprint typeset using LaTeX style emulateapj v. 5/2/11

arXiv:1402.3161v1 [astro-ph.SR] 13 Feb 2014

ANGULAR MOMENTUM EXCHANGE IN WHITE DWARF BINARIES ACCRETING THROUGH DIRECT IMPACT

J. F. Sepinsky[1] and V. Kalogera[2]
[1] The University of Scranton, Department of Physics and Electrical Engineering, Scranton, PA 18510, *jeremy.sepinsky@scranton.edu*, and
[2] Center for Interdisciplinary Exploration and Research in Astrophysics (CIERA) & Department of Physics and Astronomy, Northwestern University, 2145 Sheridan Road, Evanston, IL 60208, *vicky@northwestern.edu*

Submitted to The Astrophysical Journal

ABSTRACT

We examine the exchange of angular momentum between the component spins and the orbit in semi-detached double white dwarf binaries undergoing mass transfer through direct impact of the transfer stream. We approximate the stream as a series of discrete massive particles ejected in the ballistic limit at the inner Lagrangian point of the donor toward the accretor. This work improves upon similar earlier studies in a number of ways. First, we self-consistently calculate the total angular momentum of the orbit at all times. This includes changes in the orbital angular momentum during the ballistic trajectory of the ejected mass, as well as changes during the ejection/accretion due to the radial component of the particle's velocity. Second, we calculate the particle's ballistic trajectory for each system, which allows us to determine the precise position and velocity of the particle upon accretion. We can then include specific information about the radius of the accretor as well as the angle of impact. Finally, we ensure that the total angular momentum is conserved, which requires the donor star spin to vary self-consistently. With these improvements we calculate the angular momentum change of the orbit and each binary component across the entire parameter space of direct impact double white dwarf binary systems. We find a significant decrease in the amount of angular momentum removed from the orbit during mass transfer, as well as cases where this process increases the angular momentum of the orbit at the expense of the spin angular momentum of the donor. We conclude that, unlike earlier claims in the literature, mass transfer through direct impact need not destabilize the binary and that the quantity and sign of the orbital angular momentum transfer depends on the binary properties, particularly the masses of the double white dwarf binary component stars. This stabilization may significantly impact the population synthesis calculations of the expected numbers of events/systems for which double white dwarfs may be a progenitor, e.g. Type Ia supernovae, Type .Ia supernovae, and AM CVn.

Subject headings: Celestial mechanics, Stars: Binaries: Close, Stars: Mass Loss, Accretion, Methods: Numerical

1. INTRODUCTION

Double white dwarf (DWD) binaries provide an interesting key to understanding a number of different astrophysical problems. Their birth properties provide insight into the evolution of their progenitors (e.g., Nelemans et al. 2001b), as well as the dynamics of common envelope evolution (e.g., Toonen et al. 2012). From a population standpoint, DWDs may make up a large fraction of the close binary stars in our galaxy, creating a confusion limited background for high frequency space-based gravitational wave detectors such as LISA (Nelemans et al. 2001b; Ruiter et al. 2010). As these objects evolve via gravitational radiation loses (Webbink 1984; Iben & Tutukov 1984) their shrinking orbit may eventually allow them to be detected as individual systems (e.g., Nather et al. 1981; Evans et al. 1987; Hils et al. 1990; Saffer et al. 1988).

As the DWD orbit continues to shrink via gravitational radiation, the less massive component will inevitably fill its Roche lobe and the system will enter a semi-detached state. It is in this interacting phase when sources and sinks of angular momentum other than gravitational radiation become vitally important in determining the eventual fate of the system. Marsh et al. (2004) (See also Gokhale et al. 2007; Han & Webbink 1999; Kremer et al. 2014, in prep) analyze the stability of the mass transfer process for DWDs. A number of possibilities have been discussed in the literature. If the mass transfer process if unstable, the binary orbit will shrink until a merger occurs. Such a merger may create such objects as R CrB or SdB stars (e.g., Saio & Jeffery 2002). If the system is sufficiently massive, a Type Ia supernova may result (Webbink 1984; Iben & Tutukov 1984; van Kerkwijk et al. 2010; Toonen et al. 2012). Mergers of low-mass white dwarfs have also been proposed as the origin of Type .Ia supernovae (Shen et al. 2010; Kilic et al. 2013), where the properties of the binary immediately prior to merger can significantly affect the observed characteristics of such explosion (van Kerkwijk et al. 2010). In the case where the mass transfer is stable, such systems may be identifiable as AM CVn (Tutukov & Yungelson 1996; Nelemans et al. 2001a).

Three such stable double white dwarf AM CVn are thought to exist: HM Cnc, V407 Vul, and EX Cet (See Solheim 2010, and references therein). Each of these systems has an orbital period less than 12 minutes with no observable disk, making them excellent candidates

for direct impact (DI) mass transfer. Nelemans et al. (2001a) noted that, since the radius of the accretor in a DWD is large compared to the orbital separation, DI mass transfer is likely to occur. Indeed, examining the distance of closest approach for the ballistic trajectories of Lubow & Shu (1975), inserting the Roche lobe radius of Eggleton (1983) and the mass-radius relation for zero-temperature white dwarfs of Verbunt & Rappaport (1988), one finds (see Figure 1 of Marsh et al. 2004, Figure 1 of this paper) that the majority of the parameter space of DWDs will undergo DI mass transfer.

The evolution of the binary through this DI mass transfer phase crucially depends on the exchange of angular momentum between the binary components, as well as between the orbit and the component spins. Understanding this process is necessary to determine accurate rates for the creation of many of the astrophysical phenomena discussed previously.

Marsh et al. (2004) finds that, while the stability of the system is largely dependent on the unknown tidal coupling between the accretor and the orbit, the majority of DI systems will be unstable. Gokhale et al. (2007) notes that the stability of these systems may be improved if the rotation rate of the donor is allowed to vary. However, both of these studies assume that (i) the orbital angular momentum of the particle at accretion is equal to the angular momentum of the circularization radius (Verbunt & Rappaport 1988; Flannery 1975), (ii) that all the angular momentum of the particle is deposited enitrely into the spin of the accretor, and (iii) that the angular momentum change during the particle's motion can be extracted from the semi-major axis of the binary orbit. As we show here, these assumptions are not always justified. Indeed, hydrodynamic studies of close white dwarf binaries suggest that these systems my be more stable than previously expected (Motl et al. 2007; Dan et al. 2009).

In this paper, we follow the full ballistic trajectory of the ejected mass for each system, calculating the feedback onto the spin and orbital angular momenta of each star throughout the ejection, transit, and accretion process. In section 2, we describe our ballistic model and highlight the changes in the angular momenta of the donor and accretor. In section 3 we examine the total changes in the angular momenta of the system for any DWD undergoing DI mass transfer and compare to previous results. Finally, in section 4, we discuss the implications of these findings and propose a method to employ these results in future studies.

2. BALLISTIC TRAJECTORIES

In this section, we describe the ballistic models of Sepinsky et al. (2010) as used here for the particular case of DWD Roche lobe overflow DI mass transfer. Below, we highlight the portions of the calculation that are particularly important to this problem and refer the interested reader to that paper and references therein for a more general discussion of orbital evolution due to DI mass transfer.

2.1. *Basic Assumptions*

We consider a close binary system of two white dwarfs with masses M_D (donor) and M_A (accretor), volume-equivalent radii of $\mathcal{R}_D$ and $\mathcal{R}_A$, and uniform rotation rates $\vec{\Omega}_D$ and $\vec{\Omega}_A$ with axes perpendicular to the orbital plane. We assume the mass of each star is distributed spherically symmetrically. The binary is assumed to be in an initially circular Keplerian orbit with semi-major axis a and orbital period $P_{\rm orb}$. The radius of each object is assigned following Eggleton's zero-temperature mass-radius relation (equation 15 of Verbunt & Rappaport 1988). We chose the semi-major axis of the orbit such that the volume equivalent radius of the mass donor ($\mathcal{R}_D$) is equal to the volume-equivalent radius of its Roche lobe as fit by Eggleton (1983). Both the donor and accretor initially rotate synchronously with the orbit[1].

Our ballistic calculations are performed in a stationary inertial reference frame located at the initial center of mass of the binary system. From this reference frame, the positions of the centers of mass the donor and accretor are given by $\vec{R}_D$ and $\vec{R}_A$ with velocities $\vec{V}_D$ and $\vec{V}_A$, respectively.

2.2. *Ballistic Model*

We model the mass transfer as a discrete event where a particle of mass $M_P \ll M_D, M_A$ is instantaneously ejected from the inner Lagrangian point of the donor, $\vec{r}_{L_1}$ (measured from the center of mass of the donor), with velocity $\vec{V}_P$ equal to the vector sum of the donor's rotational velocity at the point of ejection, the orbital velocity of the donor, and the ejection velocity of the particle relative to the center of mass of star 1, $\vec{V}_{\rm ej}$,

$$\vec{V}_P = \vec{\Omega}_D \times \vec{r}_{L_1} + \vec{V}_D + \vec{V}_{\rm ej}. \tag{1}$$

We let $\vec{V}_{\rm ej}$ have a magnitude equal to the sound speed in a white dwarf atmosphere of temperature $20\ 000\,K$ directed along the line connecting the mass centers of the two objects. We note that, provided $|\vec{V}_{\rm ej}|/|\vec{V}_P| \lesssim 0.01$ the angular momentum exchange between the particle and the system during transport is unaffected by changes in $|\vec{V}_{\rm ej}|$.

When the particle is ejected, the center of mass of the system remains fixed. Since the particle's mass is instantaneously transported to the surface, this forces a shift in the position of the donor's center of mass. Additionally, conservation of linear and angular momentum imply a change in the donor's velocity and rotation rate, respectively. Writing these conservation laws yields the following equations for the position, velocity, and rotation rate of the donor after ejection

$$\vec{R}_{D,F} = M_{D,F}^{-1}\left(M_{D,I}\vec{R}_{D,I} - M_P\vec{R}_P\right) \tag{2}$$

$$\vec{V}_{D,F} = M_{D,F}^{-1}\left(M_{D,I}\vec{V}_{D,I} - M_P\vec{V}_P\right) \tag{3}$$

$$\vec{\Omega}_{D,F} = I_{D,F}^{-1}\left(I_{D,I}\vec{\Omega}_{D,I} + M_{D,I}\vec{R}_{D,I}\times\vec{V}_{D,I} - M_{D,F}\vec{R}_{D,F}\times\vec{V}_{D,F} - M_P\vec{R}_P\times\vec{V}_P\right) \tag{4}$$

where I_D is the moment of inertia of the donor star. The subscript "I" denotes that the quantity is considered immediately before the ejection of the particle, and

[1] If the donor rotates non-synchronously, the Roche lobe radii can be calculated as given in Sepinsky et al. (2007).

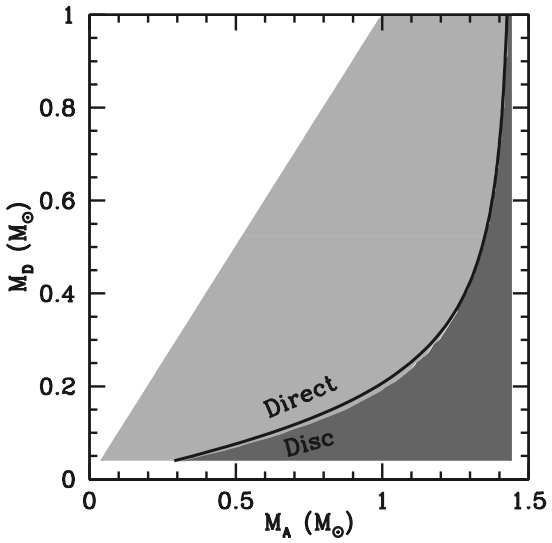

FIG. 1.— The result of a single ballistic integration as a function of the masses of the donor and accretor. Light grey points represent systems which undergo DI, while dark grey points undergo DF. The solid line represents the analytical boundary as described in Marsh et al. (2004) (See text for details).

the subscript "F" denotes the quantity immediately after ejection.

Following ejection, the trajectory of the three bodies are numerically integrated following the standard Newtonian equations of motion using an $8^{\rm th}$ order Runge Kutta ordinary differential equation solver (Galassi et al. 2006). Throughout the course of the integration, the total energy and momentum of the system are conserved to, generally, better than 1 part in 10^{12}. While there is no coupling between the spins of either component and the motion of the ejected particle, the orbital angular momentum of both donor and accretor will be affected by the transport of the particle.

During the particle's trajectory, if it ever comes closer to the accretor than its radius, i.e., $|\vec{R}_P - \vec{R}_A| < \mathcal{R}_A$, the particle accretes. When this occurs, the center of mass of the system remains fixed. Since the particle's mass is added to the accretor, this necessitates a shift in the accretor's center of mass. Additionally, conservation of linear and angular momentum imply a change in the accretor's velocity and rotation rate, respectively. To calculate the change in these quantities during accretion it is sufficient to use equations (2)–(4), simply replacing all quantities referencing the donor with the respective quantities referencing the accretor and letting $M_P \rightarrow -M_P$. In this case, the position and velocity of the particle are those immediately prior to accretion.

2.3. *Binary Parameter Space for Mass Transfer through Direct Impact*

For the purpose of this work, we are only interested in orbital changes due to ballistic trajectories where the particle impacts the surface of the accretor within one orbital period (i.e., those in which DI occurs). Following the above procedure, we compute the outcome for systems with $M_A < 1.44\,M_\odot$ and $M_D < M_A$. If the particle accretes within one orbital period, we classify this as a direct impact. If the particle does not accrete within one orbital period it is likely the ejection stream from the donor will self-intersect, resulting in the eventual formation of an accretion disc. We identify these systems as disc formation (DF) systems[2].

In Figure 1 the light grey region corresponds to systems which undergo DI, while the dark grey region corresponds to systems which undergo DF. The solid line near the boundary of these two regions is an analytical approximation to this boundary, which was first derived and presented by Marsh et al. (2004) (which itself followed a similar derivation in Nelemans et al. (2001a)). Following them, we calculate this line by taking the distance of closest approach for a ballistic trajectory given by Lubow & Shu (1975) (as analytically fit by Nelemans et al. (2001a)) and setting it equal to the radius of the accretor (as given by Eggleton's zero-temperature mass-radius relation (Verbunt & Rappaport 1988)). In calculating this line, we assume the donor (also described by the same zero-temperature mass-radius relation) completely fills its Roche lobe (Eggleton 1983). As expected, our numerical results agree quite well to this analytic approximation. We fit the transition between DI and DF as given by our numerical calculations with the equation

$$M_D = \frac{1 - 9.24 M_A + 4.75 M_A^2}{36 M_A - 54}. \qquad (5)$$

This equation is plotted as the solid black line in Figure 6.

2.4. *Angular Momentum Changes Over One Orbit*

To calculate the stability of white dwarf binary systems previous studies (e.g., Marsh et al. 2004; Gokhale et al. 2007) have focused primarily on changes in the orbital angular momentum of the system since such changes are directly associated with changes in the mass ratio and semi-major axis of the system. In those studies, the angular momentum exchange was calculated using a numerical prescription based on Verbunt & Rappaport (1988); it assumed that the angular momentum transferred from the orbit to the spin of the accretor is exactly equal to the average angular momentum of the ballistic particle during its motion from the donor to the accretor. Here we examine the angular momentum exchange between all relevant components: the two binary members and the orbit, and we find that for a certain part of the parameter space the usual assumption above does not hold. Specifically, we allow the spin of the donor to vary self-consistently[3], and we account for the feedback onto the orbit at the moments of mass ejection and accretion. We explain the derivation of the full account of angular-momentum exchange in what follows.

We begin by rewriting equations (2)–(4) in terms of the change in the position, velocity, and spin angular momentum of the donor, $\vec{J}_{{\rm Spin},D} = I_D \vec{\Omega}_D$, per unit ejected mass. To first order in the mass of the ballistic particle,

[2] We note that in Sepinsky et al. (2010) we identified a third possible outcome of this ejection scenario: Self-accretion, in which the ejected mass falls back onto the donor star. This outcome is only possible for eccentric and/or non-synchronously rotating systems, both of which lie outside the parameter space of this study.

[3] Gokhale et al. (2007) does allow for variation in the spin of the donor, but does not do so in a a self-consistent manner. They reduce the specific spin angular momentum of the donor by the specific angular momentum of the ejected mass on the surface of the star.

we find

$$\frac{\Delta\vec{R}_D}{M_P} \equiv \frac{\vec{R}_{D,F} - \vec{R}_{D,I}}{M_P} = \frac{\vec{R}_{D,I} - \vec{R}_P}{M_{D,I}} \quad (6)$$

$$\frac{\Delta\vec{V}_D}{M_P} \equiv \frac{\vec{V}_{D,F} - \vec{V}_{D,I}}{M_P} = \frac{\vec{V}_{D,I} - \vec{V}_P}{M_{D,I}} \quad (7)$$

$$\frac{\Delta\vec{J}_{\rm Spin,D}}{M_P} \equiv \frac{\vec{J}_{\rm Spin,D,F} - \vec{J}_{\rm Spin,D,I}}{M_P} = -\left(\vec{R}_{D,I} - \vec{R}_P\right) \times \left(\vec{V}_{D,I} - \vec{V}_P\right). \quad (8)$$

Since the total angular momentum of the system is conserved during ejection, it follows that

$$\Delta\vec{j}_{\rm ej} \equiv \frac{\Delta\vec{J}_{\rm orb,D}}{M_P} \equiv \frac{\vec{J}_{\rm orb,D,F} - \vec{J}_{\rm orb,D,I}}{M_P} = -\frac{\Delta\vec{J}_{\rm Spin,D}}{M_P} - \vec{R}_P \times \vec{V}_P \quad (9)$$

where $\vec{R}_P \times \vec{V}_P$ is the specific angular momentum of the ejected particle as measured by the center of mass and we define $\Delta\vec{j}_{\rm ej}$ as the change in the orbital angular momentum per unit particle mass due to the ejection of a ballistic particle.[4]

Similarly, during accretion

$$\Delta\vec{j}_{\rm ac} \equiv \frac{\Delta\vec{J}_{\rm orb,A}}{M_P} \equiv \frac{\vec{J}_{\rm orb,A,F} - \vec{J}_{\rm orb,A,I}}{M_P} = -\frac{\Delta\vec{J}_{\rm Spin,A}}{M_P} + \vec{R}'_P \times \vec{V}'_P \quad (10)$$

where $\vec{R}'_P \times \vec{V}'_P$ is the specific angular momentum of the particle immediately before accretion as measured by the center of mass and we define $\Delta\vec{j}_{\rm ac}$ as the change in the orbital angular momentum per unit particle mass due to the accretion of a ballistic particle. Equation (10) follows from rewriting equations (6)-(8) in terms of the accretor during particle impact by simply replacing all quantities referencing the donor with the respective quantities referencing the accretor and letting $M_P \to -M_P$. In that derivation, the position and velocity of the particle are those immediately prior to accretion.

Since the total angular momentum must be conserved, the orbital angular momentum of the donor and accretor must vary as the orbital angular momentum of the particle varies during its transport from donor to accretor. We do not include any coupling between the spins of the components and the particle trajectory (which could only arise due to tidal interactions between the ejected mass and the binary components), thus the orbital angular momentum is the only property affected. We write the change of orbital angular momentum per unit particle mass during during transport from donor to accretor as $\Delta\vec{j}_{\rm t}$.

[4] Alternatively, we can derive the final step of equation 9 as follows. We first write the orbital angular momentum of the donor before and after accretion as $\vec{J}_{{\rm orb},D,F} = M_{D,F}\vec{R}_{D,F} \times \vec{V}_{D,F}$ and $\vec{J}_{{\rm orb},D,I} = M_{D,I}\vec{R}_{D,I} \times \vec{V}_{D,I}$, respectively. Then, by substituting equations (6)–(8) and recognizing that $M_{D,I} - M_{D,F} = M_P$, we can reproduce equation (9) without explicitly invoking the conservation of angular momentum.

The total change in the orbital angular momentum per unit particle mass, $\Delta\vec{j}_{\rm orb,T}$, for a single ballistic trajectory is then

$$\Delta\vec{j}_{\rm orb,T} = \Delta\vec{j}_{\rm ej} + \Delta\vec{j}_{\rm t} + \Delta\vec{j}_{\rm ac} \quad (11)$$

$$= -\Delta\vec{j}_{\rm Spin,D} - \Delta\vec{j}_{\rm Spin,A}, \quad (12)$$

where $\Delta\vec{j}_{\rm Spin,D} = \Delta\vec{J}_{\rm Spin,D}/M_P$ and $\Delta\vec{j}_{\rm Spin,A} = \Delta\vec{J}_{\rm Spin,A}/M_P$ are the total change in the spin angular momentum of the donor and accretor, respectively, per unit particle mass. This statement simply represents the conservation of angular momentum throughout all aspects of the ballistic calculation.

We note that neither Marsh et al. (2004) nor Gokhale et al. (2007) include any immediate feedback on the orbit due to ejection and accretion. As such, they impose $\Delta\vec{j}_{\rm ej} = \Delta\vec{j}_{\rm ac} = 0$. This implies that all changes to the orbital angular momentum of the system must take place during the particle motion from donor to accretor. Stated another way, equations (9) and (10) show that this constraint implies that both ejection and accretion of the particle happen tangentially to the surface of the accretor, which is unlikely to be the case, particularly for the accretor (See Lubow & Shu 1975).

For the component spins, Marsh et al. (2004) assume that the donor remains tidally locked, and thus $\Delta j_{{\rm Spin},D} = 0$, while Gokhale et al. (2007) allow the spin of the donor to vary. Both papers assume that, during accretion, the orbital angular momentum of the particle is added entirely to the accretor's spin. But as equations (9)-(11) show, conservation of angular momentum then forces unrealistic constraints on the motion of the ballistic particle. Specifically, the particle must follow a trajectory that starts with and results in tangential ejection and accretion, independent of the actual dynamics of the system, and must have velocities that exactly reproduce $\Delta j_{{\rm Spin},D}$ and $\Delta j_{{\rm Spin},A}$. One should not expect such a trajectory to exist in the general case. The change in the orbital angular momentum during particle motion is independent of the change in spins, and should be calculated separately. We further enumerate the differences between our model and the previous results in section 3.3.

In this paper, we directly calculate the change in orbital angular momentum at each stage – ejection, particle motion, and accretion. While the orbital angular momentum of the particle need not be different in our two methods, the fraction of angular momentum that arises from, or is deposited into, the spin of the components may differ significantly. In the next section, we explore the exchange of angular momentum for one example system in detail.

2.5. *Angular Momenta Variations Throughout One Orbit*

In Figure 2 we show the changes in the angular momenta per unit particle mass as a fraction of the total angular momentum of the system for a single ballistic trajectory as a function of time in units of the orbital period. The system shown has $M_D = 0.1\,M_\odot$ and $M_A = 0.45\,M_\odot$. As described above, the semi-major axis was chosen such that the donor star completely fills its Roche lobe for a zero-temperature mass-radius relation. As the particle is ejected at time $t = 0$ we see an in-

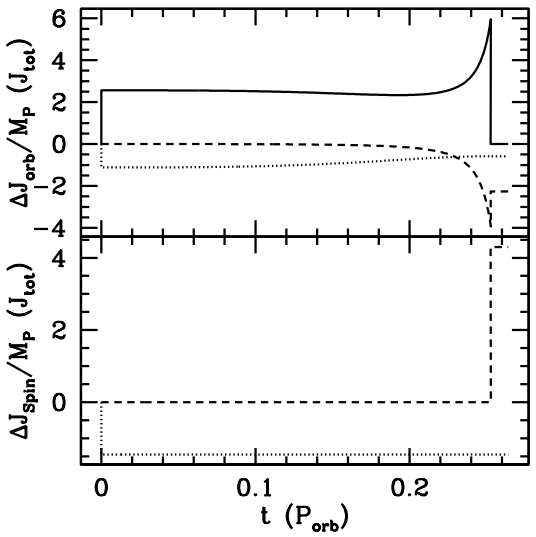

FIG. 2.— Change in the angular momenta per unit ejected mass in units of the total angular momentum of the system as a function of time in units of the orbital period for a portion of a single ballistic orbit. The shown system has a donor mass of $M_D = 0.1\,M_\odot$, accretor mass of $M_A = 0.45\,M_\odot$, and assumes the donor exactly fills its Roche lobe for a zero-temperature white dwarf mass-radius relation. At top, we show the change in orbital angular momentum of each component. At bottom we show the change in spin angular momentum of each component. The solid, dotted, and dashed lines show the changes in the angular momenta of the particle, donor, and accretor, respectively.

stantaneous decrease in the orbital angular momentum of the donor star (dotted lines), with an accompanying decrease in its spin angular momentum. The accretor's orbital and spin angular momenta (dashed lines) remain unchanged. The orbital angular momentum of the particle (solid line) increases instantaneously.

Between ejection ($t = 0$) and accretion ($t \approx 0.25$), the orbital angular momentum of the particle, donor, and accretor vary. During the first half of the particle transport ($t \lesssim 0.1$) there is very little change in any orbital angular momenta since the particle remains very close to the inner Lagrangian point of the donor, and hence the net force on the particle is small. As the particle falls towards the accretor it more than doubles its orbital angular momentum, which is removed, primarily, from the accretor. The orbital angular momentum of the donor increases slightly during this segment.

At accretion, the entirety of the particles orbital angular momentum is deposited into the accretor. But, as can be seen in the Figure, not all of that momentum is deposited into the spin of the accretor. For the system shown, the increase in the orbital angular momentum of the donor is approximately 1/2 of the increase in its spin angular momentum.

The proportion deposited into the spin versus the orbit depends directly on the angle between the normal to the surface at the point of impact and the instantaneous velocity of the particle at impact. If the particle impacts exactly radially to the surface, the particle's angular momentum is deposited only into the orbital angular momentum of the accretor. If the particle's velocity is exactly tangential to the surface at impact, then the particle's angular momentum is deposited entirely into the spin of the accretor. If the particle's velocity is at an angle neither tangential nor perpendicular to the surface, then the particle's angular momentum is distributed between the orbital and spin angular momenta as determined by equations (8)-(10).

During impact, the orbital and spin angular momenta of the donor remain unchanged.

In this example system, after a complete cycle of particle ejection from the donor, motion from donor to accretor, and accretion, the orbital angular momenta of the donor and accretor, and thus of the system as a whole, decreased. The spin angular momentum of the donor decreased, while the spin angular momentum of the accretor increased. In section 4 we show the total changes in the spin and orbital angular momentum of each object, as well as the system as a whole, across broad parameter space for Roche lobe overflow double white dwarf binaries.

We note that any changes in the orbital angular momentum in this fashion are bound to instantaneously change the eccentricity of the system. While such an eccentricity is not relevant to the results of this paper, it is reasonable to assume that since the accretion is expected to be symmetric with orbital phase any induced eccentricity will be conservatively damped, resulting in a system with the same orbital angular momentum in a circular orbit. We defer such eccentricity considerations to future investigations.

2.6. *Applicability of the Ballistic Motion Assumptions*

Finally, we note that changes in the properties of the binary due to mass transfer (equations [6]–[8]) are directly proportional to the mass of the ballistic particle. Thus, for $M_P \ll M_D, M_A$, ejection of the ballistic particle should have little to no effect on the orbital changes of immediately subsequent ballistic ejections. Provided the total amount of mass transferred remains small, the rate of change of the binary properties can be determined by multiplying equations (6)–(8) by the mass transfer rate. Even though the mass transfer rate may be high during Roche lobe overflow ($\lesssim 10^{-5}\,M_\odot\,yr^{-1}$, Marsh et al. 2004), the orbital periods are very short ($\lesssim$ hours). This implies that amount of mass ejected each orbit should be of order $M_P/M_D \approx 10^{-9}$. While the orbital parameters will not change appreciably during each orbit, they will slowly evolve on the timescale of years. Marsh et al. (2004) shows the evolution of the mass transfer rate in the case where the donor spin remains fixed (see §3.3). The evolution of the mass transfer rate given the model presented here will be presented in a forthcoming paper (Kremer et al. 2014).

3. RESULTS

3.1. *Angular Momentum Changes Due to Direct Impact Accretion*

In Figure 3 we show the change in angular momentum per unit ejected mass in units of the total angular momentum following a single ballistic orbit as a function of the donor mass. Only systems undergoing DI mass transfer as identified in Figure 1 are shown. The shaded regions of each color show the variation in systems as a function of accretor mass. Shown in cyan and magenta are the changes in the spin angular momenta per unit transferred mass of the donor ($\Delta j_{\rm Spin,D}$)

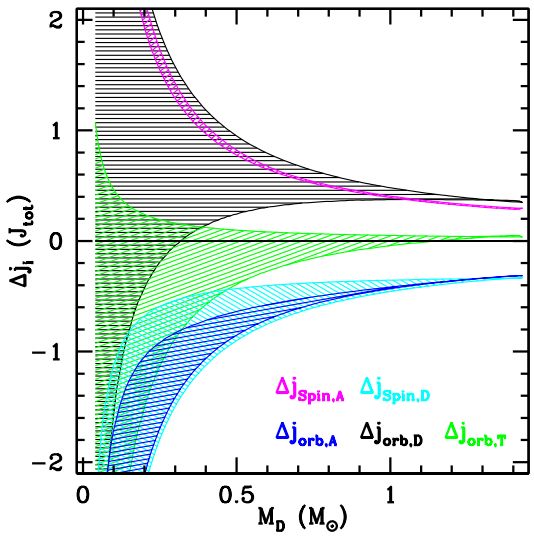

FIG. 3.— The single-orbit change in the orbital angular momentum per unit transferred mass in units of the total angular momentum as a function of the donor mass for white dwarfs undergoing DI mass transfer. For each donor mass, the vertical extent of the shaded regions correspond to variations in the accretor mass that can be seen in Figure 1. The line-shaded regions correspond to the changes in the angular momentum associated with a specific component of the system as follows: cyan and magenta are the change in the spin angular momentum per unit transferred mass for the donor and accretor, respectively; black and blue are the change in the orbital angular momentum per unit transferred mass for the donor and accretor, respectively; and green is the total change in the orbital angular momentum of the system per unit transferred mass. The solid black line consistent with $\Delta j = 0$ shows the change in the total angular momentum per unit transferred mass.

and accretor ($\Delta j_{\rm Spin,A}$), respectively; in black and blue are the changes in the orbital angular momenta per unit transferred mass of the donor ($\Delta j_{\rm orb,D}$) and accretor ($\Delta j_{\rm orb,A}$), respectively; and in green is the change in the total orbital angular momentum of the system ($\Delta j_{\rm orb,T} = \Delta j_{\rm orb,A} + \Delta j_{\rm orb,A}$). The black solid line shows the change in the total angular momentum of the system. This line is consistent with zero to better than 1 part in 10^5 throughout the parameter space and shows the accuracy of our angular momentum calculations.

A few characteristics of Figure 3 deserve more discussion.

First, we see that the change in the spin angular momentum of the accretor (magenta) is always positive. This is as expected from the literature, where the ballistic particle impacts the surface of the accretor with a tangential velocity greater than the rotational velocity at the surface of the accretor. Repeated accretion of this fashion will eventually create a rapidly rotating accretor. We see that, as the donor mass decreases, the change in the spin angular momentum of the accretor increases significantly. Furthermore, we note that this parameter has only a minor dependence on the mass of the accretor.

Next, we see that the change in the spin angular momentum of the donor (cyan) is always negative. Since the particle is being ejected from the L_1 point with velocity components due to the rotational velocity of a uniformly rotating donor at that point, the particle carries away the specific spin angular momentum of the surface of the donor plus a small contribution due to the thermal ejection velocity.

Similarly, the change in the orbital angular momentum of the accretor (blue) is always negative. The variation is due to the position of the particle impact, as well as the direction of the particle's impact velocity and the other binary properties. Additionally, there can be a significant change in the orbital angular momentum of the accretor during the particle transport, as can be seen in Figure 2.

We see that the change in the orbital angular momentum of the donor (black) can be either positive or negative, depending on both the mass of the donor and of the accretor. For a mass ratio $M_D/M_A > 0.27$, $\Delta j_{\rm orb,D}$ is always positive, though for systems $M_D/M_A < 0.27$ $\Delta j_{\rm orb,D}$ may either increase or decrease. As with the change in the spin angular momentum of the donor, this will vary based on the velocity and angle of the particle ejection. Additionally, the orbital angular momentum of the donor may change during the particle motion, as can be seen in Figure 2.

The change in the total orbital angular momentum of the system (green) can be either positive or negative, depending on both the mass of the donor and of the accretor. For a mass ratio $M_D/M_A > 0.85$, $\Delta j_{\rm orb,T} > 0$, though for systems $M_D/M_A < 0.85$ $\Delta j_{\rm orb,T}$ may either increase or decrease depending on the component masses. We discuss the implications of $\Delta j_{\rm orb,T} > 0$ in §4.

We emphasize that the approaches to this problem previously presented in the literature (i) do not include any change in the orbital angular momentum of either the donor or accretor due to the ejection or accretion of the particle; and (ii) change the orbital angular momentum of the system during particle motion by adjusting the semi-major axis instead of accounting for the changes in orbital angular momentum of either/both component stars. The results presented here do include such changes in the position and orbital and rotational velocities of both objects during ejection, particle motion, and accretion, which in turn create the observed changes in the angular momenta. We defer investigations of the eccentricity induced during this process to a future study.

We note that, as discussed in the previous section, provided the mass of the ejected particle is sufficiently small, such changes may be scaled by the desired mass transfer rate to obtain the rate of change of the desired quantity as a function of time. Furthermore, it is imperative to realize that any changes in the orbital or spin angular momenta of either component will affect any subsequent ballistic ejection, orbit, and accretion. Thus, the changes shown above are *not* a steady state solution but merely represent the initial single-orbit change for the given set of initial parameters. For an investigation of the long-term orbital changes due to the process described here, see Kremer et al. (2014)

3.2. *Angular Momentum Changes with Strong Tidal Coupling*

It is commonly assumed (Marsh et al. (2004); but see also Gokhale et al. (2007)) that the rotational velocity of the donor will remain synchronized with the orbital velocity. This is generally expected since Roche lobe overflow requires extreme tidal distortions in the donor star which act to synchronize its rotational velocity on short timescales. The accretor is generally not affected as strongly by tidal synchronization since, being more

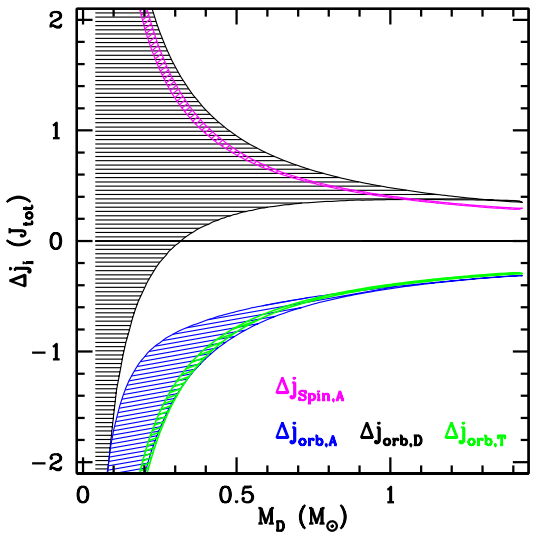

FIG. 4.— As Figure 3, but assuming the donor rotational velocity remains synchronized with the orbital velocity.

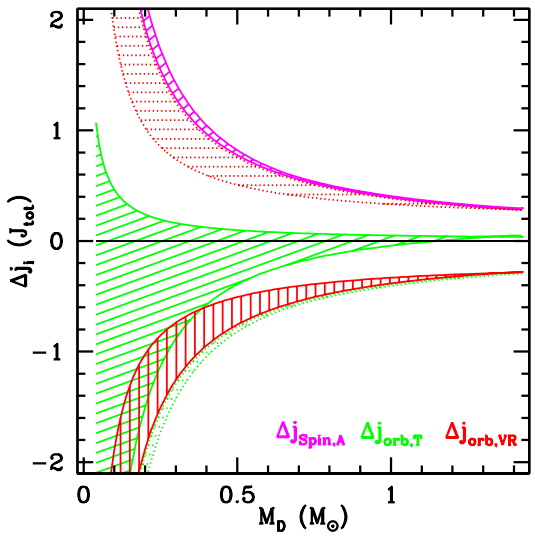

FIG. 5.— As Figure 3, but adding comparisons to the standard prescription from the literature. The green line-shaded area corresponds to the change in the total orbital angular momentum per unit transferred mass for the approach presented in §3.1. The green dot-shaded area corresponds to the change in the total orbital angular momentum per unit transferred mass for the approach presented in §3.2. The magenta line-shaded area corresponds to the change in the spin angular momentum of the accretor per unit transferred mass for the approach presented in §3.1. The red line-shaded region corresponds to the change in orbital angular momentum per unit transferred mass that would arise following the prescription of Verbunt & Rappaport (1988), while the red dot-shaded region corresponds to the change in the spin angular momentum of the accretor per unit transferred mass under the same assumptions. See text for details.

massive, it is not expected to be significantly tidally distorted. Some tidal coupling between the accretor and the orbit is generally assumed, though it is not expected to be strong enough to keep the accretor from becoming a rapid rotator.

To simulate a strong tidal coupling between the donor and the orbit, we show in Figure 4 the same results as Figure 3 except we assume the donor's rotational velocity remains synchronized to the orbital velocity. Hence, we assume the angular momentum that would be removed from the spin of the donor is immediately returned from the orbit. In Figure 4, $\Delta j_{\rm orb,T} = \Delta j_{\rm orb,D} + \Delta j_{\rm orb,A} + \Delta j_{\rm Spin,D}$. As expected, the total change in the orbital angular momentum in this case is simply the negative of the change in the spin angular momentum of the donor. The changes in the orbital angular momenta of both components remains the same as Figure 3.

3.3. *Comparison to previous results*

In Figure 5 we compare the change in the total orbital and accretor spin angular momenta per unit transferred mass for the non-synchronous and synchronous models presented earlier, as well as the change in the orbital angular momentum per unit transferred mass as presented in the literature.

The green line-shaded area shows the change in the total orbital angular momentum per unit transferred mass where we allow the spin angular momentum of the donor to change self-consistently, as shown in Figure 3. The green dot-shaded region shows the total orbital angular momentum per unit transferred mass where the rotation rate of the donor is fixed, as shown in Figure 4. The magenta line-shaded region is the change in the spin angular momentum of the accretor per unit transferred mass. The red line-shaded region shows the change in the angular momentum of the orbit per unit transferred mass used in Marsh et al. (2004) and Gokhale et al. (2007). The red dot-shaded region shows the spin angular momentum per unit transferred mass added to the accretor as used in the previous works and is simply the negative of the red dash-shaded region.

Following Marsh et al. (2004) we calculate the red dash-shaded region employing the method of Verbunt & Rappaport (1988). They begin by writing the orbital angular momentum of the transferred mass in terms of the circular orbit with the same specific angular momentum. They then use their equation (13) as their fitting formula for the radius of this orbit. The fitting formula is scaled to the semi-major axis of the orbit which we calculate by combining the fitting formula for the Roche lobe radius given by Eggleton (1983) with the fitting formula for the radius of zero-temperature white dwarfs of Eggleton (1986) (as quoted by Verbunt & Rappaport 1988), assuming the donor completely fills its Roche lobe. The fitting formula used, however, does not represent the angular momentum of the particle at impact. Instead, it is a fit to the angle-averaged radius of an ejected particle throughout a ballistic orbit as given by Lubow & Shu (1975, ϖ_d; table 2).

We see that, for most of the parameter space, the change in the total orbital angular momentum of the system is more positive than when applying the prescription of Verbunt & Rappaport (1988) (see Figure 5). Thus, it appears that mass transfer using these ballistic assumptions may have less of a destabilizing affect that previously expected. Furthermore, since there are areas of the parameter space where $\Delta j_{\rm orb,T} > 0$, mass transfer may *increase* the stability of the orbit.

In Figure 6 we show the changes in the orbital angular momentum per unit transferred mass in the parameter space of Figure 1. As in Figure 1, the dark grey region in the lower right corresponds to systems which undergo DF. The remainder of the parameter space are

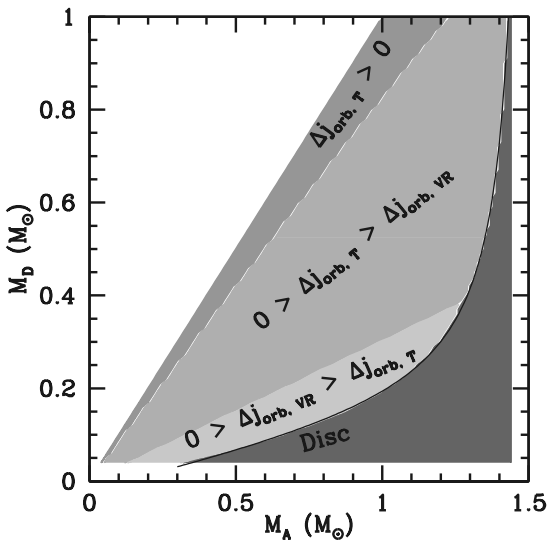

FIG. 6.— As Figure 1, but we further divide the DI parameter space into regimes based on the net change in orbital angular momentum following a ballistic ejection, particle motion, and accretion. The darkest grey region undergoes DF. In the DI regime, from darkest to lightest, the regions represent: (1) where the total orbital angular momentum increases, (2) where the total orbital angular momentum decreases by an amount less than that assumed by previous studies, (3) where the total orbital angular momentum decreases by a greater amount than that assumed by previous studies. The thin black line shows the fit for the transition between DI and DF given by equation 5.

systems which undergo DI, which we further subdivide, from darkest to lightest, as follows: (1) systems where the total orbital angular momentum increases; (2) systems where the total orbital angular momentum decreases, but at a slower rate than previously assumed in the literature; (3) systems where the total orbital angular momentum decreases more rapidly than previously assumed in the literature. The dividing lines between each region are nearly, but not quite, linear. The dividing line between regions (1) and (2) has a slope of approximately $M_D/M_A \approx 0.825$, while the dividing line between regions (2) and (3) has a slope of approximately $M_D/M_A \approx 0.30$. Thus, the change in the total orbital angular momentum appears to become more positive with increasing donor mass.

Curiously, this stability is directly opposite that seen in previous investigations. The analysis of Marsh et al. (2004, e.g., Figure 1) shows that systems with a low donor mass are more likely to remain stable over long periods of time, while the majority of the parameter space (depending on the strength of the tidal coupling) is expected to be unstable. Here, by including the additional mass transfer effects presented here in a self-consistent way, DWD DI mass transfer may induce a stabilizing effect over a larger area of the parameter space. Indeed, as seen in Figure 6, the region furthest from the stability region of Marsh et al. (2004) receives the largest stabilizing effect, where the orbital angular momentum of the system is *increased* due to DI mass transfer. As can be seen from Figure 3, this increased orbital angular momentum arises at the expense of the spin angular momentum of the donor and the ejection velocity of the ejected mass, which provides a small impulse to the center of mass of the donor, pushing it to a larger orbit and increasing its orbital angular momentum. The net effect of DI mass transfer, when tracking the orbital angular momentum of the system in detail, is a system more stable than that expected following the assumptions in the current literature.

4. DISCUSSION

We have shown that, if one takes into account the changes in both the spin and orbital angular momenta of the component stars during mass ejection/accretion, as well as numerically calculating the ballistic model for each mass transfer scenario, the resultant transfer of angular momentum can be significantly different than the result currently described in the literature. In many cases the orbital angular momentum lost from the orbit can be significantly less than the standard assumption, making this process less destabilizing than expected. This may allow for more DWD to survive the semi-detached state and become AM CVn, instead of merging to create Type Ia or Type .Ia supernovae. This may have significant implications on population synthesis models of these objects.

In a few cases, we have shown that mass transfer may *increase* the orbital angular momentum of the orbit, thereby providing a stabilizing effect on the orbit. We caution again that the results presented here are for a single mass transfer event over a single binary orbit, and thus do not represent a steady state solution. Nevertheless, any stabilizing effect increases the chances of a long-lived semi-detached DWD, lending credence to the creation of AM CVn through the DWD scenario.

In order to analyze changes in the long-term stability of these systems, we will incorporate our ballistic calculations into a long term numerical integration, taking into account tides and gravitational radiation. By updating the ballistic trajectories and angular momentum changes at every timestep, we will be able to self-consistently calculate the long-term evolution of the system conserving the total angular momentum from ejection to accretion. Results from these calculations will be presented in a forthcoming paper (Kremer et al. 2014).

The authors acknowledge many useful conversations and debates which helped to shape the work into its present form, particularly those with Tom Marsh, Bart Willems, Paul Groot, Danny Steeghs, Gijs Nelemans, and Juhan Frank. This project was supported in part by an internal faculty research grant from the University of Scranton to JS, a Simons Fellowship in Theoretical Physics to VK. VK is also grateful for the hospitality of the Aspen Center for Physics where part of this work was completed.

REFERENCES

Dan, M., Rosswog, S., & Brüggen, M. 2009, Journal of Physics Conference Series, 172, 012034
Eggleton, P. P. 1983, ApJ, 268, 368
Evans, C. R., Iben, Jr., I., & Smarr, L. 1987, ApJ, 323, 129
Flannery, B. P. 1975, MNRAS, 170, 325

Galassi, M., J., D., Theiler, J., Gough, B., Jungman, G., Booth, M., & Rossi, F. 2006, GNU Scientific Library Reference Manual (2nd Ed.) (Network Theory Ltd.)
Gokhale, V., Peng, X. M., & Frank, J. 2007, ApJ, 655, 1010
Han, Z., & Webbink, R. F. 1999, A&A, 349, L17
Hils, D., Bender, P. L., & Webbink, R. F. 1990, ApJ, 360, 75
Iben, Jr., I., & Tutukov, A. V. 1984, ApJS, 54, 335
Kilic, M., Hermes, J. J., Gianninas, A., Brown, W. R., Heinke, C. O., Agueros, M. A., Chote, P., Sullivan, D. J., Bell, K. J., & Harrold, S. T. 2013, ArXiv e-prints
Kremer, K., Sepinsky, J. F., & Kalogera, V. 2014, ApJ
Lubow, S. H., & Shu, F. H. 1975, ApJ, 198, 383
Marsh, T. R., Nelemans, G., & Steeghs, D. 2004, MNRAS, 350, 113
Motl, P. M., Frank, J., Tohline, J. E., & D'Souza, M. C. R. 2007, ApJ, 670, 1314
Nather, R. E., Robinson, E. L., & Stover, R. J. 1981, ApJ, 244, 269
Nelemans, G., Portegies Zwart, S. F., Verbunt, F., & Yungelson, L. R. 2001a, A&A, 368, 939
Nelemans, G., Yungelson, L. R., & Portegies Zwart, S. F. 2001b, A&A, 375, 890
Ruiter, A. J., Belczynski, K., Benacquista, M., Larson, S. L., & Williams, G. 2010, ApJ, 717, 1006
Saffer, R. A., Liebert, J., & Olszewski, E. W. 1988, ApJ, 334, 947
Saio, H., & Jeffery, C. S. 2002, MNRAS, 333, 121
Sepinsky, J. F., Willems, B., & Kalogera, V. 2007, ApJ, 660, 1624
Sepinsky, J. F., Willems, B., Kalogera, V., & Rasio, F. A. 2010, ApJ, 724, 546
Shen, K. J., Kasen, D., Weinberg, N. N., Bildsten, L., & Scannapieco, E. 2010, ApJ, 715, 767
Solheim, J.-E. 2010, PASP, 122, 1133
Toonen, S., Nelemans, G., & Portegies Zwart, S. 2012, A&A, 546, A70
Tutukov, A., & Yungelson, L. 1996, MNRAS, 280, 1035
van Kerkwijk, M. H., Chang, P., & Justham, S. 2010, ApJ, 722, L157
Verbunt, F., & Rappaport, S. 1988, ApJ, 332, 193
Webbink, R. F. 1984, ApJ, 277, 355

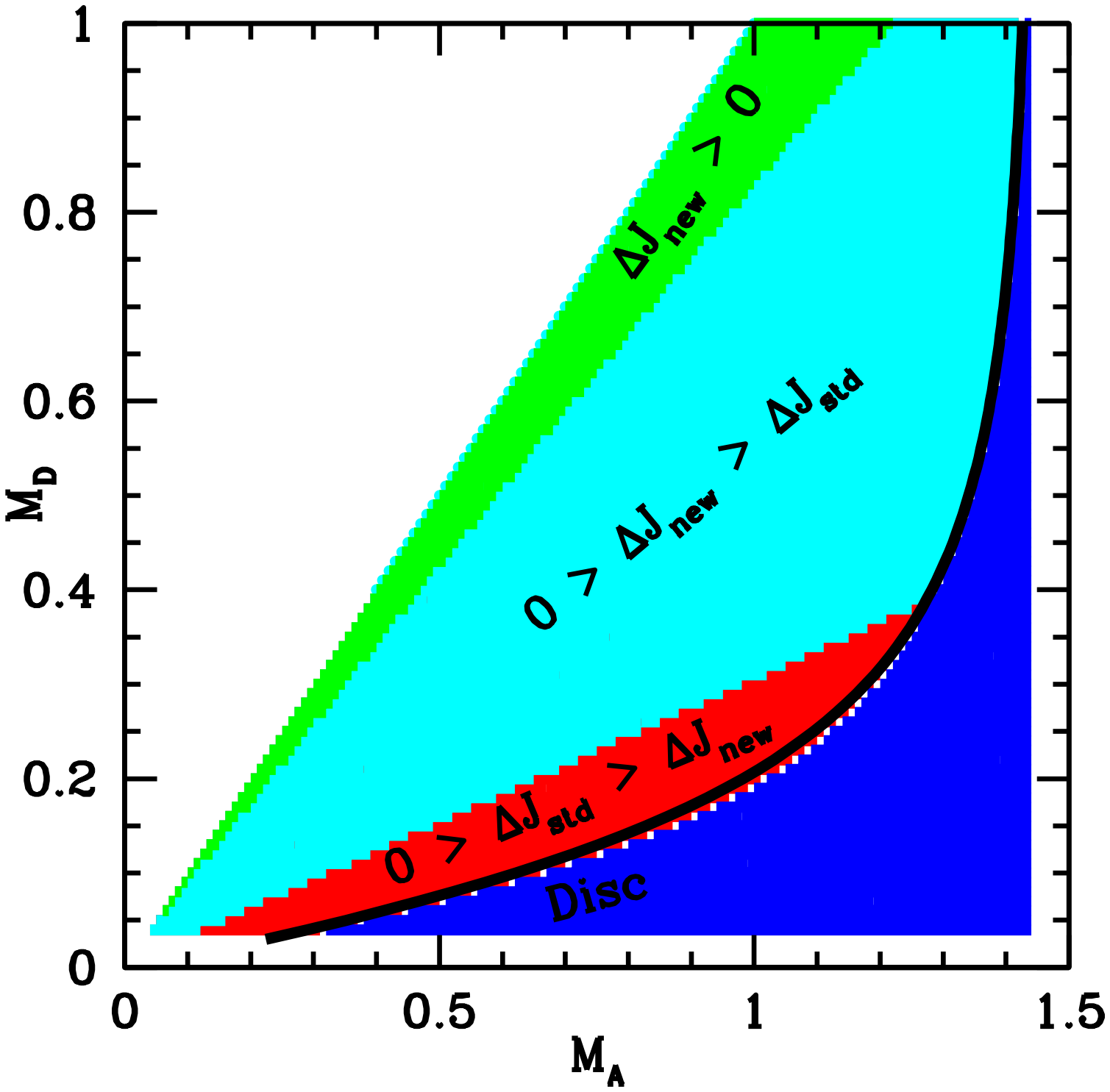
1
0.8
0.6
0.4
0.2
0
M_D
0
0.5
1
1.5
M_A
$\Delta J_{new} > 0$
$0 > \Delta J_{new} > \Delta J_{std}$
$0 > \Delta J_{std} > \Delta J_{new}$
Disc